



## Single Layer Dual Circularly Polarized Antenna Elements for Automotive Radar at 77 GHz

Downloaded from: <https://research.chalmers.se>, 2025-12-04 23:23 UTC

Citation for the original published paper (version of record):

Zang, Z., Uz Zaman, A., Yang, J. et al (2021). Single Layer Dual Circularly Polarized Antenna Elements for Automotive Radar at 77 GHz. 15th European Conference on Antennas and Propagation, EuCAP 2021. <http://dx.doi.org/10.23919/EuCAP51087.2021.9411028>

N.B. When citing this work, cite the original published paper.

# Single Layer Dual Circularly Polarized Antenna Elements for Automotive Radar at 77 GHz

Zhaorui Zang<sup>1</sup>, Ashraf Uz Zaman<sup>1</sup>, Jian Yang<sup>1</sup>, Carlo Bencivenni<sup>2</sup>, Konstantinos Konstantinidis<sup>3</sup>

<sup>1</sup> Department of Electrical Engineering, Chalmers University of Technology, Gothenburg, Sweden,

zhaorui.zang@chalmers.se

<sup>2</sup> Gapwaves AB, Gothenburg, Sweden

<sup>3</sup> Veoneer Germany GmbH, Niederwerrn, Germany

**Abstract**—In this paper, two different configurations of dual circularly polarized antenna elements in single layer gap waveguide (GW) are presented for 77GHz automotive radar systems. Both of the antenna configurations utilize slot element to radiate and generate circular polarizations. The right-hand circular polarization (RHCP) and the left-hand circular polarization (LHCP) are generated at the same working frequency with different input ports. The simulated results show that both two antenna elements could cover the proposed impedance bandwidth (75-80 GHz) with an axial ratio lower than 2 dB.

**Index Terms**—slot antenna, dual circularly polarized antenna, gap waveguide, millimeter wave.

## I. INTRODUCTION

Recently, 77 GHz radars have been investigated and used in automotive Advanced Driver Assistance Systems (ADAS) for detecting and imaging of objects and targets [1,2]. These radars need to be robust and compact in size, which are essential for such applications. However, most of them lack the ability to precisely perceive the complicated environment on the road. One way to improve the detection capability of a radar system is to use polarimetric technique. Polarimetric radars always use dual linearly polarized (LP)/ circularly polarized (CP) electromagnetic waves to classify targets near the vehicles [3]. The motivation of using dual-polarization is to capture extra features of the targets which have been missed or neglected by a single polarized radar. For some specially-shaped small targets, the cross-section may be so tiny that single polarization (LP) systems have difficulties to detect them. Dual-polarization can solve this problem to some extent theoretically, by analyzing the correlations of the transmitted signals and received signals with different polarizations from the target [4,5]. Furthermore, automotive vehicles are expected to run on the road regardless the weather and road conditions. So, radars are expected to be able to detect water, ice, oil or other different road surfaces in order to change the driving strategy or route for the sake of safety. Circular polarization has been widely used in remote and weather satellites to discern rain, snow and melting layer for a long time. Therefore, dual circular-polarization is a better choice to perceive more information from surroundings for automotive vehicles.

Several millimeter wave (mmWave) circularly polarized antennas have been reported recently [6-8]. Most of them are substrate-based arrays with a small aperture. Because of the material property, substrates have always substantial dielectric losses at high frequencies. To solve this problem, many waveguide slot arrays has been designed [9-12]. However, due to the small wavelength at 77GHz, the size of conventional all metal waveguide becomes so small that it is hard to be manufactured precisely with a reasonable manufacturing cost.

Gap waveguide (GW) technology has been proven to be a good candidate to solve the dielectric loss and manufacturing problem [13]. GW is a new waveguide structure based on soft and hard surface theory. The working principle of GW is to create a stop-band within a parallel waveguide made by a PEC (metal) and PMC (plate with periodic pins). The whole structure can be made of metal, eliminating dielectric loss. In addition, GW is easier and cheaper to be manufactured by using conventional low-cost manufacturing [14,15]. There have been several designs of circularly polarized antenna based on GW [16-19]. In [18], a low profile  $4 \times 4$  single layer array is designed. The antenna has a simple structure and is fed by a combination of ridge gap waveguide (RGW) and groove gap waveguide (GWG), showing the possibility of large array design. In [19], a 3-layer high- gain RHCP antenna is realized. The whole antenna array is excited by sequential-phase feeding network and has 21.8% axial ratio ( $< 3\text{dB}$ ) bandwidth and 23.5 dBi gain. However, both of them are only for single circular polarization and need complex geometries for developing a dual CP array.

Low-manufacture-cost and simple structured dual circularly polarized antenna with good performance are demanded. Many advanced feeding strategies, such as two orthogonal feedings, a sequential-phase feeding network, or a hybrid coupler, are often employed to generate and improve CP performance. However, these feeding strategies need either complex feeding structure, often in a multilayer structure, or complicated signal processing. As a result, the whole structure of a dual circularly polarized antenna would be more complex.

In this paper, two types of dual fed dual-CP-polarization antenna elements, realized on a single layer GW, have been investigated and designed. The structures of these antennas

are presented in Section II and the simulation results are presented in Section III.

## II. ANTENNA DESIGNS

The two antenna elements are designed to operate at the frequency band of 75-80 GHz. Both of them have only one waveguide layer, fed by RWG. The top plate of the RGW has a slot for radiation and the bottom plate is implemented with a ridge and periodic pins for feeding the slot. Periodic pins are placed at both sides of the ridges, as a PMC boundary, to generate stop-band and secure electromagnetic waves propagating along the ridge.

### A. Design of configuration A: U-shaped slot

The U-shaped slot configuration is shown in Fig. 1. The square slot is cut in the center of the top metal plate and fed by two ridges along y-axis. The slot and the feeding lines are asymmetric in x-axis direction to generate circular polarization. By tuning the K1, K2, and F2 parameters, the axial ratio performance can be optimized. Here an equal value of L and W is chosen to reduce the coupling between the two ports. The ridge's height has been changed with step to improve the isolation between the two ports also.

The proposed antenna radiates an RHCP wave when port 1 is excited. If the input is at port 2, an LHCP wave is radiated. The whole structure is realized by metal. The optimized values of the parameters of configuration A are shown in Table 1.

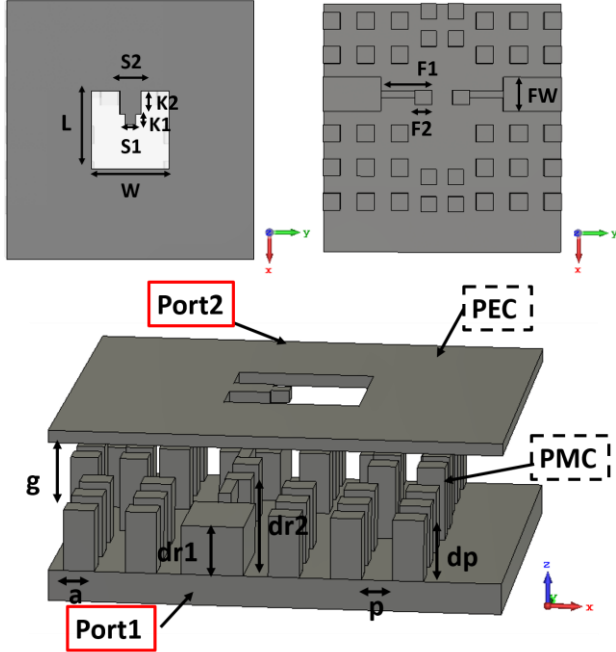


Fig. 1. Structure of configuration A

### B. Design of configuration B: X-shaped slot

Fig. 2 shows the structure of configuration B. It is designed based on an X-shaped slot. The slot is placed on the top metal plate and fed by a ridge gap waveguide section. Instead of placing in the center of the top plate, there is an offset for the slot from the ridge center. This asymmetry is critical to have a good CP performance. Along the x-axis direction, the distance between the two sides of the ridge is set at one wavelength. The dual CP is realized by feeding different sides of the ridge. When port 1 is excited, an RHCP wave is radiated. When port 2 is excited, an LHCP is radiated. The parameters values of antenna B are shown in Table 2.

TABLE I. PARAMETERS OF ANTENNA A

Par.	S1	S2	K1	K2	L	W	F1	F2
Val(mm)	0.3	0.8	0.3	0.56	2.2	2.2	1.5	0.5
Par.	FW	a	p	dp	dr1	dr2	g	
Val(mm)	1	0.5	0.5	0.9	0.65	0.95	0.12	

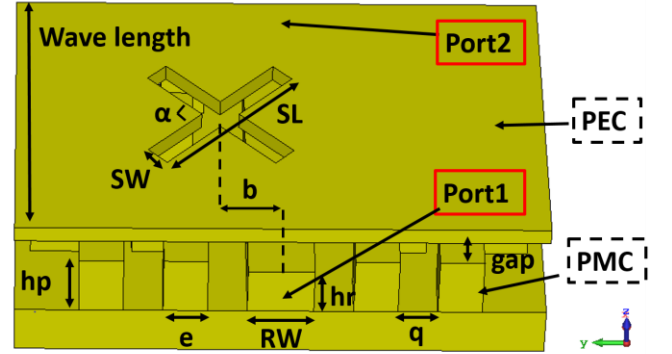


Fig. 2. Structure of configuration B

TABLE II. PARAMETERS OF ANTENNA B

Par.	SL	SW	RW	e	b
Val(mm)	2.02	0.3	0.75	0.5	0.4
Par.	q	hr	hp	gap	$\alpha$
Val(mm)	0.45	0.6	0.75	0.1	90°

## III. SIMULATION RESULTS

The proposed two antenna configurations are simulated by CST Microwave Studio 2019. The thickness of top metal plate is 0.2 mm.

### A. Results of configuration A

The simulated S-parameters of configuration A are shown in Fig. 3. Within the bandwidth of 75-80 GHz, the  $S_{11}$  is lower than -15.6 dB. The port coupling is below -15.9 dB in the operating bandwidth. The  $S_{12}$  has same value as  $S_{21}$  because the structure has a symmetry plane in x-z plane. Similarly,  $S_{22}$  and  $S_{11}$  share the same value.

Fig. 4 illustrates the radiation pattern of the proposed configuration at  $\varphi=0$  degree plane and  $\varphi=90$  degree plane, when port 1 is excited (RHCP is realized). In z-axis direction, the difference between LHCP and RHCP is 27.6 dB. The directivity of the configuration A is 6.63 dBi.

The axial ratio is presented in Fig. 5, which is below 0.88 dB within the impedance bandwidth.

### B. Results of configuration B

As shown in Fig.6, the reflection coefficient is below -21.8 dB, and the port coupling is lower than -3.4 dB within proposed working band (75-80 GHz). Similar to configuration A,  $S_{21}$  and  $S_{12}$ ,  $S_{11}$  and  $S_{22}$  have the same value.

The radiation pattern of proposed configuration at the plane of  $\varphi=0$  degree and  $\varphi=90$  degree is illustrated in Fig.7. When port 1 is excited, a RHCP is realized by the X-shaped slot. In z-axis direction, the difference between LHCP and RHCP is about 22.4 dB. The directivity of the antenna configuration B is 5.2 dBi.

As shown in Fig. 5, the axial ratio of configuration B is below 2.1 dB within 75-80 GHz.

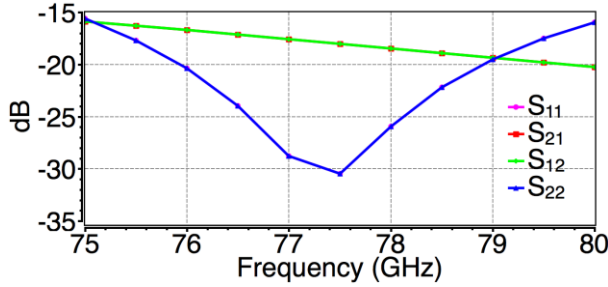


Fig. 3. The S-parameters of configuration A

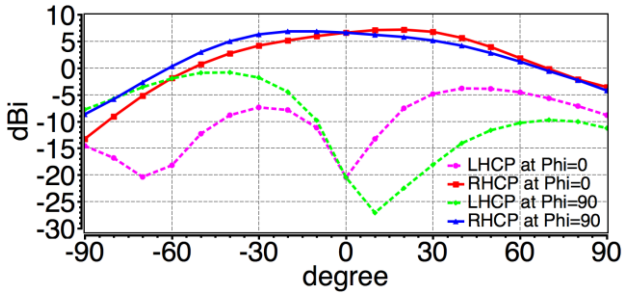


Fig. 4. Radiation pattern of configuration A at 77 GHz

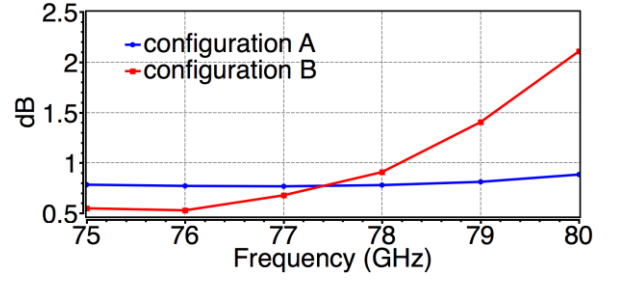


Fig. 5. Axial ratio of configuration A and configuration B

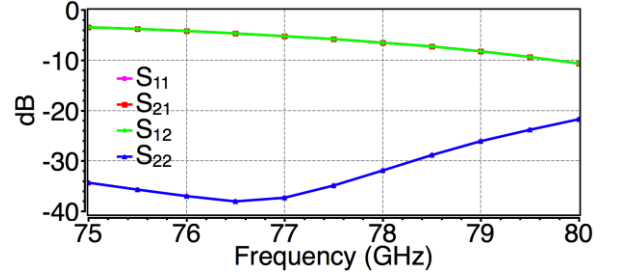


Fig. 6. The S-parameters of configuration B

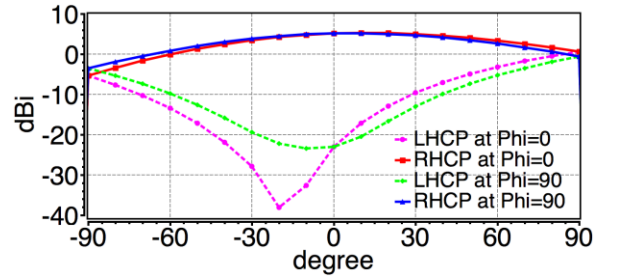


Fig. 7. Radiation pattern of configuration B at 77 GHz

The comparison of two configurations is shown in Table III. Impedence band width is not discussed here since the proposed working band (75-80 GHz) is not so wide and both the proposed antenna configuration cover this frequency band.

TABLE III. COMPARISON BETWEEN TWO CONFIGURATIONS

	$S_{21}$ (dB)	AR (dB)
configuration A	< -15.9	< 0.88
configuration B	< -3.4	< 2.1

For  $S_{21}$ , configuration B is lower than configuration A. The result is reasonable because B is supposed to work in a travelling wave array, where  $S_{21}$  just presents the percent of microwave energy transmitted to the next element. In other words, more energy would be radiated and  $S_{21}$  would be improved by adding more elements in the array. For Axial

ratio, configuration A has better circularly polarization purity at the proposed working band. On the other hand, Configuration B has a more compact structure than configuration A and shows promising features for realizing a planar array.

#### IV. CONCLUSIONS

In this paper, two configurations of dual circularly polarized antenna element are designed and simulated based on GW technology. Both of them realize a reflection coefficient lower than -15 dB and an axial ratio lower than 2 dB in the proposed frequency range (75-80 GHz). These configurations have compact structure, ease of integration and low cost in manufacturing. The two configurations are promising candidates for future automotive radar modules.

#### ACKNOWLEDGMENT

The authors would like to thank Esparanza Alfonso from Gapwaves AB, Olof Eriksson from Veoneer Sweden, Robert Moestam and Bo Wendemo from CEVT for their support and discussion during this project. This work is supported by Swedish Strategic Vehicle Research and Innovation FFI grant 2018-02707.

#### REFERENCES

- [1] X. Cai and K. Sarabandi, "A Machine Learning Based 77 GHz Radar Target Classification for Autonomous Vehicles," in 2019 IEEE International Symposium on Antennas and Propagation and USNC-URSI Radio Science Meeting, 2019: IEEE, pp. 371-372.
- [2] A. A. Belyaev, I. O. Frolov, T. A. Suanov, and D. O. Trots, "Object Detection in an Urban Environment Using 77GHz Radar," in 2019 Radiation and Scattering of Electromagnetic Waves (RSEMW), 2019: IEEE, pp. 436-439.
- [3] T. Visentin, *Polarimetric Radar for Automotive Applications*. KIT Scientific Publishing, 2019.
- [4] S. Trummer, G. F. Hamberger, U. Siart, and T. F. Eibert, "A polarimetric 76-79 GHz radar-frontend for target classification in automotive use," in 2016 46th European Microwave Conference (EuMC), 2016: IEEE, pp. 1493-1496.
- [5] G. F. Hamberger, S. Späth, U. Siart, and T. F. Eibert, "A mixed circular/linear dual-polarized phased array concept for automotive radar—planar antenna designs and system evaluation at 78 GHz," *IEEE Transactions on Antennas and Propagation*, vol. 67, no. 3, pp. 1562-1572, 2018.
- [6] Y.-H. Yang, B.-H. Sun, and J.-L. Guo, "A low-cost, single-layer, dual circularly polarized antenna for millimeter-wave applications," *IEEE Antennas and Wireless Propagation Letters*, vol. 18, no. 4, pp. 651-655, 2019.
- [7] R. Kazemi, S. Yang, S. H. Suleiman, and A. E. Fathy, "Design Procedure for Compact Dual-Circularly Polarized Slotted Substrate Integrated Waveguide Antenna Arrays," *IEEE Transactions on Antennas and Propagation*, vol. 67, no. 6, pp. 3839-3852, 2019.
- [8] J. Xu, W. Hong, Z. H. Jiang, and H. Zhang, "Low-Cost Millimeter-Wave Circularly Polarized Planar Integrated Magneto-Electric Dipole and Its Arrays With Low-Profile Feeding Structures," *IEEE Antennas and Wireless Propagation Letters*, vol. 19, no. 8, pp. 1400-1404, 2020.
- [9] G. Montisci, "Design of circularly polarized waveguide slot linear arrays," *IEEE Transactions on Antennas and Propagation*, vol. 54, no. 10, pp. 3025-3029, 2006.
- [10] S. Chatterjee and A. Majumder, "Design of circularly polarized waveguide crossed slotted array antenna at Ka band," in 2015 International Conference on Microwave and Photonics (ICMAP), 2015: IEEE, pp. 1-2.
- [11] M. Salari and M. Movahhedi, "A new configuration for circularly polarized waveguide slot antenna," in Asia-Pacific Microwave Conference 2011, 2011: IEEE, pp. 606-609.
- [12] X. Wu, F. Yang, F. Xu, and J. Zhou, "Circularly polarized waveguide antenna with dual pairs of radiation slots at Ka-Band," *IEEE Antennas and Wireless Propagation Letters*, vol. 16, pp. 2947-2950, 2017.
- [13] E. Rajo-Iglesias, M. Ferrando-Rocher, and A. U. Zaman, "Gap waveguide technology for millimeter-wave antenna systems," *IEEE Communications Magazine*, vol. 56, no. 7, pp. 14-20, 2018.
- [14] A. Vosoogh, A. Haddadi, A. U. Zaman, J. Yang, H. Zirath, and A. A. Kishk, "W-Band Low-Profile Monopulse Slot Array Antenna Based on Gap Waveguide Corporate-Feed Network," *IEEE Transactions on Antennas and Propagation*, vol. 66, no. 12, pp. 6997-7009, 2018.
- [15] A. Vosoogh, M. S. Sorkherizi, A. U. Zaman, J. Yang, and A. A. Kishk, "An integrated Ka-band diplexer-antenna array module based on gap waveguide technology with simple mechanical assembly and no electrical contact requirements," *IEEE Transactions on Microwave Theory and Techniques*, vol. 66, no. 2, pp. 962-972, 2017.
- [16] J. Xi, B. Cao, H. Wang, and Y. Huang, "A novel 77 GHz circular polarization slot antenna using ridge gap waveguide technology," in 2015 Asia-Pacific Microwave Conference (APMC), 2015, vol. 3: IEEE, pp. 1-3.
- [17] M. Al Sharkawy and A. A. Kishk, "Wideband beam-scanning circularly polarized inclined slots using ridge gap waveguide," *IEEE Antennas and Wireless Propagation Letters*, vol. 13, pp. 1187-1190, 2014.
- [18] M. Ferrando-Rocher, J. I. Herranz-Herruzo, A. Valero-Nogueira, and A. Vila-Jiménez, "Single-layer circularly-polarized Ka-band antenna using gap waveguide technology," *IEEE Transactions on Antennas and Propagation*, vol. 66, no. 8, pp. 3837-3845, 2018.
- [19] M. Akbari, A. Farahbakhsh, and A.-R. Sebak, "Ridge gap waveguide multilevel sequential feeding network for high-gain circularly polarized array antenna," *IEEE Transactions on Antennas and Propagation*, vol. 67, no. 1, pp. 251-259, 2018.